Experimental Implementation of the Quantum Baker's Map

Yaakov S. Weinstein,[1] Seth Lloyd,[2,*] Joseph Emerson,[1] and David G. Cory[1]

[1]*Department of Nuclear Engineering, Massachusetts Institute of Technology, Cambridge, Massachusetts 02139*

[2]*d'Arbeloff Laboratory for Information Systems and Technology, Massachusetts Institute of Technology, Department of Mechanical Engineering, Cambridge, Massachusetts 02139*

(Received 15 January 2002; published 24 September 2002)

This Letter reports on the experimental implementation of the quantum baker's map via a three bit nuclear magnetic resonance quantum information processor. The experiments tested the sensitivity of the quantum chaotic map to perturbations. In the first experiment, the map was iterated forward and then backward to provide benchmarks for intrinsic errors and decoherence. In the second set of experiments, the least significant qubit was perturbed in between the iterations to test the sensitivity of the quantum chaotic map to controlled perturbations. These experiments can be used to investigate existing theoretical predictions for quantum chaotic dynamics.

DOI: 10.1103/PhysRevLett.89.157902 PACS numbers: 03.67.Lx, 05.45.Mt, 76.60.Pc

Chaos is a phenomenon in which nonlinear dynamical systems exhibit heightened sensitivity to small perturbations [1–8]. The study of chaos is computationally intensive. When direct experiments are not available, computers can be used to simulate chaotic dynamics and to calculate the effect of perturbations. But when the chaotic system is quantum mechanical, simulating its dynamics on a classical computer is notoriously difficult: the computational complexity of the calculation rises exponentially with the number of degrees of freedom of the simulated quantum chaotic system and with the accuracy to which the simulation is to take place [4,9,10]. If one can simulate quantum chaos on a quantum computer, by contrast, the computational complexity rises only as a small polynomial in the number of degrees of freedom and in the accuracy [10–12]. Consequently, quantum computation represents a potentially powerful technique for investigating quantum chaos. This Letter reports on an experimental demonstration of a quantum chaotic map.

Small perturbations to the initial state of a classical chaotic system typically lead to large changes in behavior. Two states that are initially close are driven apart at a rate governed by the positive Lyapunov exponents [1] of the chaotic dynamics. By contrast, quantum dynamics, whether regular or chaotic, preserves the overlap between quantum states and does not drive them apart. Nonetheless, quantum chaos can be characterized by the sensitivity of the time evolution of states to small changes in the Hamiltonian that governs the chaotic dynamics [6–8,13,14].

We implement experimentally an approach suggested by Ballentine and Zibin [13] to explore the correspondence between classical and quantum chaotic dynamics. We evolve our quantum system forward in time under the quantum baker's map, perturb it, and evolve it backward by the inverse map. The total evolution is then $\rho_i \rightarrow \rho_f = \sum_k QB^\dagger A_k QB \rho_i QB^\dagger A_k^\dagger QB$, where ρ is the density matrix of the system, QB is the unitary transformation corresponding to the quantum baker's map, and A_k are Kraus operators giving a perturbation whose strength can be varied. Finally, we compare the final state ρ_f with the initial state ρ_i for different perturbation strengths. The sensitivity of the system to the perturbations can be characterized by the overlap $\mathrm{Tr}(\rho_i \rho_f)$.

Our approach also allows for a confirmation of the ideas of Zurek and Paz [14] who suggest that quantum chaotic systems, when decohered by their environment, produce information at a rate equal to their Kolomogorov-Sinai entropy.

Further applications of our experimental methods could be used to test the criteria for quantum chaotic dynamics of Peres and of Schack and Caves. Peres [6,7] noted that under quantum chaotic dynamics with a slight perturbation, a state moves apart at an exponential rate from the same state evolving under the unperturbed dynamics. Schack and Caves [8] characterized chaotic dynamics (both classical and quantum) in terms of the exponential growth of the information required to specify a state that evolves according to a perturbed version of the dynamics, a phenomenon they termed "hypersensitivity to perturbation."

The quantum information processor used to simulate perturbed quantum chaotic maps is an NMR quantum information processor [15,16]. The number of quantum bits used (three) is sufficiently small that the precision of the quantum computation can be checked on a classical computer. Of course, the small number of qubits means that the simulation could have been performed on a classical computer. The goal of the research reported here was to actually simulate quantum chaos on a quantum information processor [17]. A further goal of experimental investigations is to identify practical experimental signatures of quantum chaos.

The classical baker's map acts on the unit square in phase space as follows:

$$\begin{aligned} q' &= q/2, \qquad p' = p/2; \qquad 0 < q < 1/2, \\ q' &= 2q - 1, \qquad p' = (p+1)/2; \qquad 1/2 \le q < 1. \end{aligned} \tag{1}$$

The baker's map first stretches phase space to twice its length, while squeezing it to half its height. Then the map cuts phase space in half vertically and stacks the right portion on top of the left portion, similar to the way a baker kneads dough. Because of the stretching and the cut, the baker's map is fully chaotic and has two Lyapunov exponents, $\pm \ln 2$. Balazs and Voros [19,20] presented a quantized version of the baker's map that reproduces the behavior of the classical map in the limit $\hbar \to 0$. The quantum baker's map is a simple unitary operator which consists of a quantum Fourier transform (QFT) on half of the Hilbert space followed by an inverse QFT on the whole Hilbert space:

$$QB_q = \mathrm{QFT}_q^{-1} \begin{pmatrix} \mathrm{QFT}_{q/2} & 0 \\ 0 & \mathrm{QFT}_{q/2} \end{pmatrix}, \tag{2}$$

where q is the Hilbert space dimension. The QFT is a discrete Fourier transform acting on a Hilbert space in the computational basis and is defined as [21]

$$\mathrm{QFT}_q |x\rangle = \frac{1}{\sqrt{q}} \sum_{x'=0}^{q-1} e^{2\pi i x x'/q} |x'\rangle. \tag{3}$$

The QFT, and hence, the quantum baker's map, can be expressed as a sequence of two basic unitary operations, the Hadamard gate, H_j, operating on spin j and the conditional phase gate, $B_{jk}(\theta)$, which applies a phase of θ on spin k if spin j is in state $|1\rangle$. Schack [12] utilized this decomposition to develop an algorithm for simulating the quantum baker's map on a quantum computer. The three qubit version of the quantum baker's map is (reading from left to right)

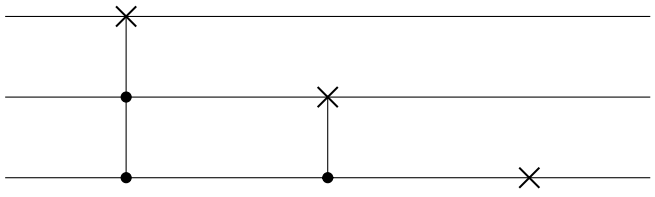

FIG. 1. Gate sequence for the three bit position perturbation. The top line, bit one, is the most significant bit. The first gate (a controlled-controlled-NOT or Toffoli gate) flips the most significant bit only if the other two bits are $|1\rangle$. The second gate (a controlled-NOT gate) flips the second bit only if the third bit is a $|1\rangle$, and the final gate is a NOT on the third bit. This sequence can be extended to an arbitrary number of qubits. Using geometric algebra [29], we can break down this sequence into NMR implementable operators; the Toffoli gate, $e^{i(\pi/8)(1-\sigma_x^1-\sigma_z^2-\sigma_z^3+\sigma_x^1\sigma_z^2+\sigma_x^1\sigma_z^3+\sigma_z^3\sigma_z^3-\sigma_x^1\sigma_z^2\sigma_z^3)}$, the controlled-NOT gate, $e^{i(\pi/4)(1-\sigma_x^2-\sigma_z^3+\sigma_x^2\sigma_z^3)}$, and the NOT gate, $e^{i(\pi/2)(1-\sigma_x^3)}$.

$$\mathrm{Swap}_{13} H_3 B_{23}^{\dagger}(\tfrac{\pi}{2}) B_{13}^{\dagger}(\tfrac{\pi}{4}) H_2 B_{12}^{\dagger}(\tfrac{\pi}{2}) H_1 \times \mathrm{Swap}_{23} H_3 B_{23}(\tfrac{\pi}{2}) H_2 \tag{4}$$

where Swap_{jk} is a swap gate between bits j and k. The second term in Eq. (4) implements a QFT on bits 2 and 3 and the first term implements the inverse QFT on all three bits [21]. Brun and Schack [11] introduced a simplified version of the baker's map and simulated, on a classical computer, its implementation on a quantum information processor. In this Letter we implement the complete baker's map defined in Eq. (4). Swap gates are done by relabeling bits.

As noted above, our experimental technique is to apply the quantum baker's map, apply a perturbation such as the position perturbation of Fig. 1, then apply the inverse map. We began most of our simulations in the pseudopure state corresponding to the state $|000\rangle$. In general, the perturbed dynamics of a single state may not be sufficient to completely characterize the behavior of a map. Here, we take advantage of the fact that the overlap $\mathrm{Tr}(\rho_i \rho_f)$ for the $|000\rangle$ initial state approaches the average of overlaps for a complete set of orthogonal initial states in the limit of small perturbation, as shown in Fig. 2. Thus the overlap

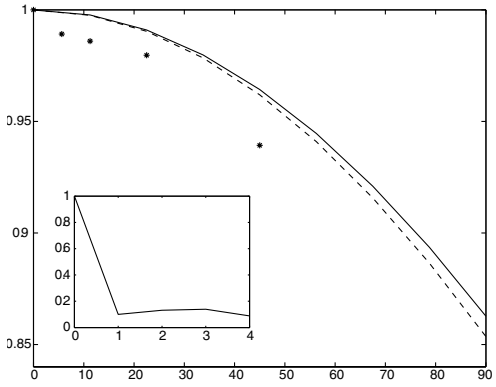

FIG. 2. Sensitivity of baker's map to unitary perturbations. Solid line shows the theoretical overlap $\mathrm{Tr}(\rho_i \rho_f)$ versus the angle of the perturbation rotation on the third bit for the initial state $|000\rangle$. The dashed curve shows the final state overlap for the same perturbation averaged over a complete set of orthonormal initial states. These curves are calculated by numerically applying the map and perturbations to the initial state. For small perturbations the results for the initial state $|000\rangle$ are very similar to that of a complete set of initial states. Stars represent the measured overlap $\mathrm{Tr}(\varrho_i \varrho_f)$ for the initial state $|000\rangle$ where ϱ_i is the state of the system after experimental implementation of the quantum baker's map followed by the inverse quantum baker's map, and ϱ_f is the state of the system after the experimental implementation of the quantum baker's map, the rotation perturbation, and the inverse quantum baker's map. The drop in overlap relative to the theoretical curve results from imperfections in the initial experimental state. The inset plot is the overlap versus the size of the position perturbation (add 1 through add 4). The baker's map is much more sensitive to a position space perturbation than to a rotation perturbation on the least significant bit.

$\mathrm{Tr}(\rho_i \rho_f)$ for the initial state $|000\rangle$ approaches the fidelity [22,23] of the operation: baker's map, rotation perturbation, inverse baker's map. We note that a complete readout of the state of the system, as done in the present work, does not scale efficiently with the number of qubits. Methods for efficient measurement of the overlap are discussed in [24,25].

An interesting nonunitary perturbation is the application of a magnetic field gradient dephasing the least significant (third) bit. The Hamiltonian of a gradient on spin j is $H_g^j(z) = e^{i\gamma(dB_z/dz)z(\sigma_z^j/2)}$, where γ is the spins gyromagnetic ratio. The gradient acts as a rotation of varying magnitude across the sample. This perturbation looks like decoherence when the signal from the entire sample is measured, effectively tracing over position z.

When simulating a quantized classical map, a natural perturbation is one with a simple definition in phase space, such as a displacement in position. The quantum baker's map, as defined by Eq. (2), associates the discretized position basis on the unit square [19] with the computational basis. The smallest possible position perturbation in a Hilbert space of dimension N corresponds to the addition or subtraction of $1(\mathrm{mod}N)$ which, for example, would take the state $|000\rangle$ to $|001\rangle$ or $|111\rangle$, see Fig. 1. Simulated data in the inset of Fig. 2 shows that, as expected, the baker's map is very sensitive to such a perturbation.

A variation of this perturbation with a simple interpretation in Hilbert space is an x rotation on one bit. A 180° rotation of the least bit on the $|000\rangle$ state gives the same output as one step of the position perturbation. The sensitivity of the baker's map to the σ_x perturbation may be examined experimentally by controlling the angle of the rotation.

The three bit quantum baker's map was implemented via NMR using the three carbon-13 spins of an alanine sample. The resonant frequency of carbon-13 on a 300 MHz spectrometer is approximately 75.468 MHz. Frequency differences between the spins are 9456.5 Hz between spins 1 and 2, 2594.3 Hz between spins 2 and 3, and 12050.8 Hz between spins 1 and 3. Coupling constants between the three spins are $J_{12} = 54.2$ Hz, $J_{23} = 35.1$ Hz, and $J_{13} = -1.2$ Hz. Relaxation time T_1 for the three carbon spins in alanine are all longer than 1.5 s, while the T_2 relaxation times are longer than 400 ms. The pulse sequences for realizing the H_j and B_{jk} gates and the implementation of the QFT as a sequence of these gates can be found in [26]. The pulse sequence for the complete quantum baker's map was compressed by relabeling bits instead of performing the swaps explicitly. Readout was done using quantum state tomography as described in [22].

To measure the accuracy with which the transformations were performed, we used the attenuated correlation measure introduced in [27,28], which is appropriate for almost fully mixed density matrices:

$$C = \left(\frac{\mathrm{Tr}(\varrho_{\mathrm{theory}} \varrho_{\mathrm{exp}})}{\sqrt{\mathrm{Tr}(\varrho_{\mathrm{theory}}^2)}\sqrt{\mathrm{Tr}(\varrho_{\mathrm{exp}}^2)}} \right) \sqrt{\frac{\mathrm{Tr}(\varrho_{\mathrm{exp}}^2)}{\mathrm{Tr}(\varrho_{\mathrm{initial}}^2)}}. \quad (5)$$

Here ϱ is the measured deviation density matrix. This does not include the large identity term in the actual high temperature liquid state, but does include a small, uniquely determined amount of the identity operator necessary for reconstructing a positive state operator. The amount of identity included is fixed for each set of experiments [22,28]. If the theoretical and experimental deviation density matrices were correlated $C = 1$, if they were uncorrelated $C = 0$, and if they were anticorrelated $C = -1$.

The first experiment consisted of two iterations of the quantum baker's map, a forward iteration followed by the inverse of the map, starting from the $|000\rangle$ pseudopure state. The attenuated correlation, C, of the implementation of the forward map is 0.76, and for the forward followed by the inverse, 0.56. The factor in parentheses in the attenuated correlation, Eq. (5), measures the correlation between theoretical and experimental density matrices without accounting for reduction in signal over the course of the experiment. This gives a crude measure of the map's accuracy in the absence of decoherence. For the forward map this unattenuated correlation is 0.93 and for the forward followed by the inverse, 0.90. Since the experiment was done on the $|000\rangle$ pseudopure state, we expect the final state of the system to be that same state. The density matrix of the spin system after the forward and inverse iteration is shown in Fig. 3.

Another set of experiments were done to explore the dynamics of the baker's map under perturbations as described above. The first perturbation experimentally tested consisted of a dephasing gradient on the third, least significant, bit. This can be done by applying a gradient which dephases all of the bits. A π pulse is then done on the first two spins, followed by another gradient pulse of the same strength. The π pulse causes the dynamics of the first gradient pulse to be undone by the second gradient pulse; hence, the effect of the gradient is only seen by the third bit (a second π pulse is done on the first two spins to put them back in their original state). We measured $C = 0.78$ for the state after the gradient and $C = 0.65$ for the state after the inverse map. For these correlation values, the loss of magnetization due to the gradient is taken into account in the normalization of $\varrho_{\mathrm{initial}}$. The final state (after the gradient and inverse map) shows the generation of one bit of entropy as seen by the equilibration of the $|000\rangle$ and $|001\rangle$ populations, as displayed in Fig. 3. This is consistent with the Paz-Zurek model for the effect of decoherence on a quantum chaotic map: when decohered, the map produces one bit of entropy per iteration, an amount equal to the Kolmogorov-Sinai entropy of the map.

In a final set of experiments rotational perturbations of $\pi/32$, $\pi/16$, $\pi/8$, and $\pi/4$ on the third (least significant)

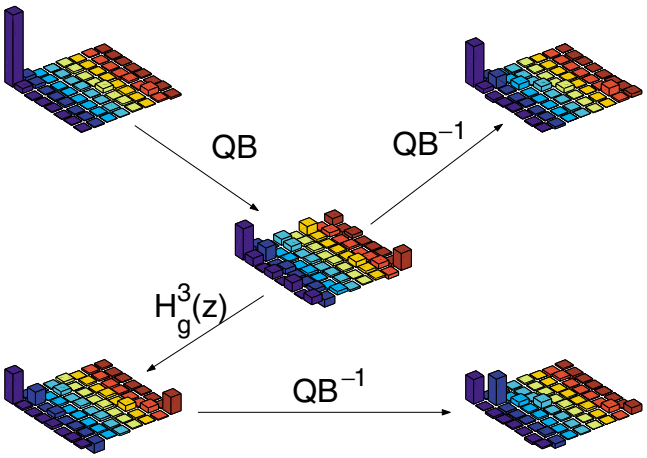

FIG. 3 (color online). Real part of experimental density matrices. The top left hand corner shows the input $|000\rangle$ pseudo-pure state. One iteration of the baker's map on this state leads to the center density matrix. Then the inverse map is applied (top right figure) bringing the bits back to the input $|000\rangle$ state. In the second experiment, a gradient is applied to the third, least significant, bit after the forward iteration of the map (bottom left figure) followed by the application of the inverse map (bottom right figure).

bit were applied between the forward and inverse iterations of the baker's map. For these experiments C ranged between 0.52 and 0.53. In Fig. 2 we plot the overlap, $\mathrm{Tr}(\varrho_i \varrho_f)$, of the experimental perturbed and unperturbed density matrices and compare it to theoretical predictions.

In conclusion, we describe the implementation of a chaotic map on a quantum system, a three qubit quantum information processor. In addition, we have explored two perturbations and examined their effects on the dynamics of the map. For small quantum systems it is more difficult to find easily implementable perturbations (one or two bit rotations) that are largely noncommuting with the map. The implemented quantum baker's map is not sensitive to the least bit rotation perturbation. However, it is sensitive to other perturbations, such as the described position perturbation. Experiments such as these establish a foundation for further experimental investigations of quantum chaotic dynamics and the exploration of suggested theoretical approaches. For example, the hypersensitivity to perturbation suggested by Schack and Caves should be evident even on a small Hilbert space, with only a few iterations of a chaotic map [11]. To eventually observe a characteristic such as the Peres criterion [6] will require a much larger Hilbert space and many more iterations of the map. We believe the experiments performed are a first step towards a more thorough experimental investigation of these questions.

The authors thank M. A. Pravia and E. M. Fortunato for help with experimental difficulties and J. P. Paz for helpful discussions. This work was supported by DARPA/MTO through ARO Grant No. DAAG55-97-1-0342 and by the Cambridge-MIT Institute.

*Author to whom correspondence should be addressed.

[1] A. J. Lichtenberg and M. A. Lieberman, *Regular and Chaotic Dynamics* (Springer-Verlag, Berlin, 1992).
[2] M. V. Berry, Proc. R. Soc. London A **413**, 183 (1987).
[3] M. V. Berry, in *New Trends in Nuclear Collective Dynamics*, edited by Y. Abe, H. Horiuchi, and K. Matsuyanagi (Springer, Berlin, 1992), p. 183.
[4] F. Haake, *Quantum Signatures of Chaos* (Springer, New York, 1991).
[5] F. Haake, M. Kus, and R. Scharf, Z. Phys. B **65**, 381 (1987).
[6] A. Peres, in *Quantum Chaos, Quantum Measurement*, edited by H. A. Cerdeira, R. Ramaswamy, M. C. Gutzwiller, and G. Casati (World Scientific, Singapore, 1991).
[7] A. Peres, *Quantum Theory: Concepts and Methods* (Kluwer, Dordecht, 1993).
[8] R. Schack and C. M. Caves, Phys. Rev. Lett. **71**, 525 (1993); R. Schack, G. M. D'Ariano, and C. M. Caves, Phys. Rev. E **50**, 972 (1994); R. Schack and C. M. Caves, Phys. Rev. E **53**, 3387 (1996); R. Schack and C. M. Caves, Phys. Rev. E **53**, 3257 (1996).
[9] R. P. Feynman, Int. J. Theor. Phys. **21**, 467 (1982).
[10] S. Lloyd, Science **273**, 1073 (1996).
[11] T. A. Brun and R. Schack, Phys. Rev. A **59**, 2649 (1999).
[12] R. Schack, Phys. Rev. A **57**, 1634 (1998).
[13] L. E. Ballentine and J. P. Zibin, Phys. Rev. A **54**, 3813 (1996).
[14] W. H. Zurek and J. P. Paz, Physica (Amsterdam) **83D**, 300 (1995).
[15] D. G. Cory, A. F. Fahmy, and T. F. Havel, Proc. Natl. Acad. Sci. U.S.A. **94**, 1634 (1997).
[16] N. A. Gershenfeld and I. L. Chuang, Science **275**, 350 (1997).
[17] We characterize liquid-state NMR as a quantum information processor to distinguish it from a quantum computer as defined by DiVincenzo [18]. Liquid-state NMR provides a test bed for simulating quantum dynamics on small Hilbert spaces. However, it is not scalable.
[18] D. P. DiVincenzo, Fortschr. Phys. **48**, 771 (2000).
[19] N. L. Balazs and A. Voros, Ann. Phys. (N.Y.) **190**, 1 (1989).
[20] M. Saraceno, Ann. Phys. (N.Y.) **199**, 37 (1990).
[21] D. Coppersmith, IBM Research Report No. RC19642, 1994.
[22] L. Viola, E. M. Fortunato, M. A. Pravia, E. Knill, R. Laflamme, and D. G. Cory, Science **293**, 2059 (2001).
[23] D. G. Cory, M. D. Price, W. Mass, E. Knill, R. Laflamme, W. H. Zurek, T. F. Havel, and S. S. Somaroo, Phys. Rev. Lett. **81**, 2152 (1998).
[24] B. Schumacher, Phys. Rev. A **54**, 2614 (1996).
[25] J. Emerson, Y. S. Weinstein, S. Lloyd, and D. G. Cory, quant-ph/0207099.
[26] Y. S. Weinstein, M. A. Pravia, E. M. Fortunato, S. Lloyd, and D. G. Cory, Phys. Rev. Lett. **86**, 1889 (2001).
[27] E. M. Fortunato, M. A. Pravia, N. Boulant, G. Teklemariam, T. F. Havel, and D. G. Cory, J. Chem. Phys. **116**, 7599 (2002).
[28] G. Teklemariam, E. M. Fortunato, M. A. Pravia, T. F. Havel, and D. G. Cory, Phys. Rev. Lett. **86**, 5845 (2001).
[29] S. S. Somaroo, D. G. Cory, and T. F. Havel, Phys. Lett. A **240**, 1 (1998).